DOI: 10.5203/pmuser.201730580

Evaluation of Punching Shear Strength Models for Glass Fibre-Reinforced Polymer (GFRP)-Reinforced Concrete (RC) Flat Plates Subjected to Unbalanced Moment-Shear Transfer

Jordan K. Carrette[1], Ehab El-Salakawy[1]

[1]Department of Civil Engineering, University of Manitoba, Winnipeg, Canada, R3T 2N2

Corresponding Author: Jordan K. Carrette (jordan.carrette@mail.utoronto.ca)

Abstract

The provisions for the punching shear strength of glass fibre-reinforced polymer (GFRP)-reinforced concrete (RC) flat plates in the current North American and Japanese standards were investigated based on a database of experimental results of both interior and edge slab-column connections. In total, the results of 39 slab-column connections ranging extensively in their geometric and material properties were collected from the literature and analyzed to assess the accuracy and validity of the code provisions. In addition, the applicability of eight proposed analytical models from the literature was verified against the results of the dataset. It was demonstrated that the Canadian and Japanese standards provide the most consistent and accurate predictions; however, the American guidelines highly underestimate the capacities. In contrast, many of the proposed analytical models yielded inconsistent and unsafe estimates when applied to both concentrically and eccentrically loaded interior and edge connections. The assumption of a linear stress variation proposed by the eccentric shear stress model was validated for GFRP-RC edge specimens subjected to unbalanced moment-shear transfer.

Keywords: reinforced concrete, punching shear, glass fibre-reinforced polymer, slab-column connection, two-way flat plate

1 Introduction

Two-way flat plate systems are susceptible to a brittle failure mode termed 'punching shear'. In general, the application of highly localized forces to the slab results in flexural and shear stresses that initiate inclined crack propagation, which in combination with circumferential cracking around the connection periphery, can cause the column to essentially punch through the slab. This sudden drop in connection capacity can lead to a progressive collapse mechanism as adjacent columns are required to support the additional loading (Wight & MacGregor, 2011).

The punching shear behaviour of flat slabs is very complex and, despite continued investigation, the fundamental failure mechanism of slab-column connections cannot be fully described by existing theories. For this reason, many of the proposed models and current code provisions are empirically based, and in most cases are derived through regression analyses of published data (Gu et al., 2016). Moreover, the use of non-corrosive GFRP bars in lieu of conventional steel reinforcement has made predicting connection capacity significantly more difficult as their mechanical properties are very distinct from those of steel. Therefore, it is not valid to simply apply the same design formulae for both reinforcement types. Coupled with the complexities mentioned above, further uncertainty is introduced when the loading pattern shifts from concentric to eccentric in the presence of an unbalanced moment. The nature of this problem warrants further research, and so it is the aim of this report to assess the accuracy and validity of the major code provisions and proposed prediction models when applied to both concentrically and eccentrically loaded specimens. Through this comparative study, it will be shown that, despite extensive investigation, there exists no universal agreement on which factors dominate the behaviour of GFRP-RC connections subjected to unbalanced moment-shear transfer.

1.1 Review of Punching Shear Equations

The following section outlines the punching shear equations used in this assessment. Furthermore, the eccentric shear stress model for combined shear and moment transfer is presented.

1.1.1 National Standards

The Canadian standard CSA S806-12 (Canadian Standards Association, 2012) specifies that the factored shear stress resistance of concrete, v_c, due to punching shear shall be taken as the minimum of Equation 1, Equation 2, Equation 3. Where β_c is the ratio of the long side to short side of the column, λ is a parameter used to account for concrete density (equal to 1.00 for normal density), ϕ_c is the resistance factor for concrete (equal to 0.65), E_f is the modulus of elasticity of the longitudinal GFRP reinforcement (MPa), ρ_f is the flexural reinforcement ratio for GFRP, $f_c^{'}$ is the compressive strength of concrete (MPa), α_s is a parameter used to ac-

count for the location of the column within the slab (equal to 4 for interior columns, 3 for edge columns, and 2 for corner columns), d is the effective slab depth (mm), and b_o is the length of the critical shear perimeter measured a distance $d/2$ from the column face (mm).

These equations are based on the punching shear equations for steel-RC slabs as outlined in the Canadian standard CSA A23.3-04 (Canadian Standards Association, 2004). El-Gamal et al. (2005) found that the neutral axis (NA) depth of the cracked section decreases considerably after cracking due to the relatively low modulus of elasticity of GFRP bars, and consequently, the shear strength of GFRP-RC slab systems becomes highly influenced by the flexural reinforcement ratio. To account for this, the term $E_f\rho_f$, known as the axial (or elastic) stiffness, was introduced in the Canadian standard CSA S806-12 (Canadian Standards Association, 2012).

$$v_c = 0.028(1 + \frac{2}{\beta_c})\lambda\phi_c(E_f\rho_f f_c^{'})^{\frac{1}{3}} \tag{1}$$

$$v_c = 0.147(0.19 + \alpha_s\frac{d}{b_o})\lambda\phi_c(E_f\rho_f f_c^{'})^{\frac{1}{3}} \tag{2}$$

$$v_c = 0.056\lambda\phi_c(E_f\rho_f f_c^{'})^{\frac{1}{3}} \tag{3}$$

$$V_c = \frac{4}{5}\sqrt{f_c^{'}b_o c} \tag{4}$$

$$k = \sqrt{2\rho_f n_f + 9\rho_f n_f)^2} - \rho_f n_f \tag{5}$$

The American guideline ACI 440.1 R-15 (ACI Committee 440, 2015) proposed Equation **4** and Equation **5** to calculate the punching shear capacity of two-way slabs reinforced with GFRP bars. Where V_c is the ultimate punching shear capacity, c, equal to kd, is the NA depth of the cracked section (mm), k is the ratio of the NA depth to reinforcement depth, and n_f is the modular ratio (quotient of modulus of elasticity of GFRP bars, E_f, and modulus of elasticity of concrete, E_c). It should be noted that the punching shear capacity, V_c, can be transformed to the punching shear stress, v_c, by simply dividing by bd.

Equation **4** was derived from the one-way shear model developed by Tureyen & Frosch (2003) and assumes that the uncracked concrete section is the only parameter effectively resisting applied shear forces; contributions from aggregate interlock and dowel action are presumed to be negligible. Furthermore, Equation **4** implicitly considers the influence of axial stiffness on the punching shear strength by calculating the NA depth of the cracked transformed section.

The Japanese standard JSCE-97 (Japan Society of Civil Engineering, 1997) developed Equation **6**, with variables defined by Equation **7** to Equation **10**, to account for the effects of the slab size, reinforcement type and ratio, and column size on the punching shear capacity. In these equations, f_{pcd} is the design compressive strength of concrete (MPa), γ_b is a safety factor set equal to 1.3, E_s is the modulus of elasticity of steel (MPa), and u is the perimeter of the loaded area (mm). Coefficients β_d, β_p, and β_r take into consideration the effect of slab depth, reinforcement ratio and type, and loaded area (column size) on the punching shear strength, respectively. The design compressive strength of concrete is calculated using Equation **10** and cannot exceed the imposed limit of 1.2 MPa and therefore does not consider the effect of high-strength concrete (HSC) on punching shear capacity.

$$v_c = \beta_d\beta_p\beta_r \times \frac{f_{pcd}}{\gamma_b} \tag{6}$$

$$\beta_d = \sqrt[4]{\frac{1000}{d}} \leq 1.5 \tag{7}$$

$$\beta_p = \sqrt[3]{100\rho_f\frac{E_f}{E_s}} \leq 1.5 \tag{8}$$

$$\beta_r = 1 + \frac{1}{1 + 0.25\frac{u}{d}} \tag{9}$$

$$f_{pcd} = 0.2\sqrt{f_c^{'}} \leq 1.2 \tag{10}$$

1.1.2 Additional Improvements

The Institute of Structural Engineers (IStructE, 1999), a British organization, recommended substitution of the steel reinforcement ratio with an equivalent GFRP ratio (or equivalent area of steel), defined as the product of the flexural reinforcement ratio (or actual GFRP reinforcement area) and the modular ratio (Equation **11**).

This GFRP ratio (Equation **11**) was substituted into the original punching shear equation for steel-RC slabs (Equation **12**) outlined in the British standard BS 8110-97 (British Standards Institution, 1997), to yield the modified version applicable for GFRP-RC slabs (Equation **13**). In these equations, ρ_s is the steel reinforcement ratio, f_{ck} is the cube concrete compressive strength (equal to $f_c^{'}/0.80$), and $b_{1.5}$ is

the length of the critical shear perimeter measured a distance $1.5d$ from the column face.

El-Ghandour et al. (1999) modified the ACI 318-95 (ACI Committee 318, 1995) punching shear equation for steel-reinforced flat slabs by introducing the cubic root of the modular ratio, or $(E_f/E_s)^{1/3}$. Equation **14** shows the original code equation and Equation **15** shows the modified version, which now accounts for the influence of flexural reinforcement on the punching shear capacity. Based on their experimental work with GFRP flat slabs, El-Ghandour et al. (2000) proposed a modification to the equivalent GFRP ratio (Equation **11**), through the inclusion of a strain correction factor (Equation **16**), where 0.0045 is the imposed strain limit for the GFRP reinforcement, and ϵ_y is the yield strain for the steel reinforcement. Substitution of Equation **16** into Equation **12** yields the revised formula (Equation **17**).

$$\rho_s = \rho_f \frac{E_f}{E_s} \tag{11}$$

$$V_c = 0.79(100\rho_s)^{\frac{1}{3}}(\frac{400}{d})^{\frac{1}{4}}(\frac{f_{ck}}{25})^{\frac{1}{3}}b_{1.5}d \tag{12}$$

$$V_c = 0.79(100\rho_f \frac{E_f}{E_s})^{\frac{1}{3}}(\frac{400}{d})^{\frac{1}{4}}(\frac{f_{ck}}{25})^{\frac{1}{3}}b_{1.5}d \tag{13}$$

$$V_c = 0.33\sqrt{f_c'}b_o d \tag{14}$$

$$V_c = 0.33\sqrt{f_c'}(\frac{E_f}{E_s})^{\frac{1}{3}}b_o d \tag{15}$$

$$\rho_s = \rho_f \frac{E_f}{E_s}\frac{0.0045}{\epsilon_y} \tag{16}$$

$$V_c = 0.79(100\rho_f \frac{E_f}{E_s}\frac{0.0045}{\epsilon_y})^{\frac{1}{3}}(\frac{400}{d})^{\frac{1}{4}}(\frac{f_{ck}}{25})^{\frac{1}{3}}b_{1.5}d \tag{17}$$

Further modification of the British standard BS 8110-97 (British Standards Institution, 1997) was made by Matthys & Taerwe (2009) who proposed Equation **18**. This revision improves the prediction accuracy as it accounts for the relatively low modulus of elasticity of GFRP reinforcement by incorporating the equivalent reinforcement ratio (Equation **11**).

Ospina et al. (2003) proposed an empirical equation based on Equation **18**, which takes the square root of the modular ratio as opposed to the cubic root and omits the size effect factor, $(1/d)^{1/4}$. Based on the available test data, Ospina et al. (2003) found it unnecessary to correct the predicted punching shear capacity, by reducing it, to account for the size effect. Additionally, they observed that the square root of the modular ratio produced more accurate results than the cubic root, therefore justifying Equation **19**.

Zaghloul & Razaqpur (2004) recommended Equation **20** based on the one-way shear equation outlined in the previous version of the Canadian standard CSA S806-02 (Canadian Standards Association, 2002).

El-Gamal et al. (2005) observed that the punching shear strength is increased when the boundary conditions restrain the slab edges against movement. They found that the amount of slab restraining is dependent on the axial stiffness of the reinforcement, the in-plane stiffness of adjacent slabs, and the presence of a supporting beam at the slab edge. Based on their conclusions, El-Gamal et al. (2005) made modifications (Equation **21**–Equation **22**) to the ACI 318-05 (ACI Committee 318, 2005) code equation. Here, α is a factor to account for the axial stiffness of the reinforcement and is a function of the effective slab depth to critical shear perimeter ratio (d/b_o). Additionally, the effect of the boundary conditions on punching shear capacity is considered by multiplying Equation **14** by 1.2^N, where N is the slab continuity factor (equal to 0 for one span in both directions, 1 for slabs continuous along one direction, and 2 for slabs continuous along both directions).

$$V_c = 1.36\frac{(100\rho_f \frac{E_f}{E_s} f_c')^{\frac{1}{3}}}{d^{\frac{1}{4}}}b_{1.5}d \tag{18}$$

$$V_c = 2.77(\rho_f f_c')^{\frac{1}{3}}\sqrt{\frac{E_f}{E_s}}b_{1.5}d \tag{19}$$

$$v_c = 0.07\lambda\phi_c(f_c'\rho_f E_f)^{0.333}b_o d \tag{20}$$

$$V_c = 0.33\sqrt{f_c'}b_o d\alpha(1.2)^N \tag{21}$$

$$\alpha = 0.62(\rho_f \frac{E_f}{1000})^{\frac{1}{3}}(1 + \frac{8d}{b_o}) \tag{22}$$

The development of a purely analytical model to predict the ultimate punching shear strength of two-way slabs is hindered by the inherent complexities of the punching

shear problem. As mentioned previously, due to the three-dimensional nature of the problem, unknown shear transfer mechanisms and unknown contributions from the uncracked concrete, aggregate interlock, and dowel action at failure render the laws of statics and mechanics ineffective. Theodorakopoulos & Swamy (2008a) developed a unified design model which encompasses their former theories for steel-RC (Theodorakopoulos & Swamy, 2002) and GFRP-RC (Theodorakopoulos & Swamy, 2007) slab-column connections. This model is unique in that it was developed without the need for empirically-derived coefficients and considers the ultimate punching shear capacity of the slab to be governed by the moment-shear interaction of the flexural and shear critical sections.

Theodorakopoulos & Swamy (2007) extended their existing steel-RC model (Theodorakopoulos & Swamy, 2002) to be applicable for GFRP-RC slabs by accounting for differences in material properties and the bond-slip behaviour between the GFRP reinforcement and concrete matrix (Equation 23–Equation 24). In these equations, V_{uf} is the ultimate theoretical punching shear strength of GFRP slabs, f_{ct} is the tensile splitting strength of concrete (equal to $0.27f_{cu}^{2/3}$), θ is the angle of failure of the fracture cone surface (assumed to be 30°), ξ_s is a size effect factor (as expressed in Equation 24), b_p is the length of the critical shear perimeter measured a distance $1.5d$ from the column face, and $(X)_f$ is the combined NA depth for GFRP slabs. The authors argued that a larger critical shear perimeter would adequately account for the shear resistance provided by the aggregate interlock and dowel action.

Theodorakopoulos & Swamy (2002) further proposed that two NA depths exist within the slab section; namely, the depth of the compression zone of the flexural section, $(X_f)_f$, and the depth of the compression zone of the shear section, X_s. The former corresponds to the location of the inclined shear cracks, whereas the latter corresponds to the location of the flexural cracks. It is hypothesized that the ultimate punching shear capacity is governed by the interaction between the moment and shear of these two critical sections. The combined NA depth (Equation 25) is represented by the harmonic mean of the flexural and shear critical section depths.

Based on experimental data for steel-RC slabs (Theodorakopoulos & Swamy, 2002), it was proposed that the depth of the compression zone of the shear critical section be taken as Equation 26.

$$V_{uf} = f_{ct}cot(\theta)\xi_s b_p (X)_f \tag{23}$$

$$\xi_s = (\frac{100}{d})^{\frac{1}{6}} \tag{24}$$

$$(X)_f = \frac{2X_s(X_f)_f}{X_s + (X_f)_f} \tag{25}$$

$$X_s = 0.25d \tag{26}$$

$$\frac{(X_f)_f^*}{d} = \frac{\epsilon_{cu}}{\epsilon_{cu} + \epsilon_f^*} \tag{27}$$

$$\frac{(X_f)_f^*}{d} = \frac{\rho_f f_f}{k_1 f_{cu}} \tag{28}$$

$$\frac{\epsilon_f}{\epsilon_{fu}} = 0.55\times [\frac{-\epsilon_{cu}/\epsilon_{fu} + \sqrt{(\epsilon_{cu}/\epsilon_{fu})^2 + 4(1+\epsilon_{cu}/\epsilon_{fu})/(\rho_f/\rho_{fb})}}{2}] \tag{29}$$

Assuming a perfect bond between the GFRP reinforcement and the hardened concrete matrix, the condition of strain compatibility and force equilibrium yields the relationships shown by Equation 27 and Equation 28, respectively (Theodorakopoulos & Swamy, 2007).

To account for the case where bond-slip occurs between the GFRP reinforcement and hardened concrete matrix, the actual GFRP strain, ϵ_f, is taken to be a fraction of the GFRP strain calculated under the assumption of a perfect bond, ϵ_f^*. Based on the available literature addressing the bond characteristics of GFRP, Theodorakopoulos & Swamy (2007) ultimately proposed a 45% reduction in the actual GFRP strain, yielding Equation 29.

Finally, the depth of the NA of the flexural section can be determined using Equation 30 in conjunction with the value found from Equation 29. Theodorakopoulos & Swamy (2008b) further simplified their GFRP model by introducing two new parameters, α_f and λ_f. The refined model for GFRP-RC slabs is expressed by Equation 31, where V_{ufd} is the ultimate design punching strength of GFRP slabs, and α_f and λ_f are design parameters expressed by Equation 32 and Equation 33, respectively. The former parameter, α_f, considers the axial stiffness of the reinforcement, $\rho_f E_f$, the ultimate design tensile strain of GFRP, $\epsilon_{fud} = 3\epsilon_{cu} = 0.0105$, and the concrete cube strength, f_{cu}. It can be proven that α_f is essentially the ratio of the flexural reinforcement ratio, ρ_f, to the balanced flexural reinforcement ratio, ρ_{fb}. The latter

parameter, λ_f, considers the bond-slip strain reduction coefficient, k_f, and is itself a function of α_f. Together, these two parameters form the simplified expression for the combined NA depth shown in Equation **34**.

For the sake of generality, Theodorakopoulos & Swamy (2008b) subsequently modified their existing steel-RC model (Theodorakopoulos & Swamy, 2002) to include the design parameters α_s and λ_s, shown by Equation **36** and Equation **37**–Equation **38**, respectively. The ultimate design punching strength of steel-RC slabs, V_{usd}, is found by evaluating Equation **35**. It can easily be seen by comparison of Equation **31** (GFRP-RC design model) with Equation **35** (steel-RC design model), that both proposed equations retain the same structure, and together result in what Theodorakopoulos & Swamy (2008b) term their 'unified design method'.

Both models use an identical expression for the combined NA, as shown by Equation **34**, from which it is concluded that the ultimate punching shear capacity is dependent on the moment-shear interaction of the two critical sections. Furthermore, Equation **34** suggests that the flexural reinforcement ratio and the concrete strength do not exist as separate entities, but rather are co-dependent. This is contrary to many of the proposed prediction models outlined previously.

$$\begin{aligned}\frac{(X_f)_f}{d} &= \frac{\rho_f E_f}{k_1 f_{cu}}\epsilon_f \\ &= \frac{\rho_f E_{fu}}{k_1 f_{cu}}\frac{\epsilon_f}{\epsilon_{fu}} \\ &\text{for } \frac{\rho_f}{\rho_{fb}} \geq 0.33\end{aligned} \tag{30}$$

$$\begin{aligned}V_{ufd} &= \frac{1}{2}0.234 f_{cu}^{\frac{2}{3}}\xi_s \frac{2\alpha_f\lambda_f}{1+\alpha_f\lambda_f}b_p d \\ &\text{for } \alpha_f > 0.33\end{aligned} \tag{31}$$

$$\begin{aligned}\alpha_f &= \frac{\rho_f f_{fud}}{0.145 f_{cu}} \\ &= \frac{\rho_f E_f \epsilon_{fud}}{0.145 f_{cu}}\end{aligned} \tag{32}$$

$$\begin{aligned}\lambda_f &= \frac{\epsilon_f}{\epsilon_{fud}} \\ &= \frac{k_f}{6}(-1+\sqrt{1+\frac{48}{\alpha_f}}) < 1 \\ &\text{for } \alpha_f > 0.33\end{aligned} \tag{33}$$

$$(X)_f = \frac{2\alpha_f\lambda_f}{1+\alpha_f\lambda_f}(0.25d) \tag{34}$$

$$V_{usd} = \frac{1}{2}0.234 f_{cu}^{\frac{2}{3}}\xi_s \frac{2\alpha_s\lambda_s}{1+\alpha_s\lambda_s}b_p d \tag{35}$$

$$\alpha_s = \frac{\rho_s f_y}{0.145 f_{cu}} \tag{36}$$

$$\lambda_s = \frac{f_s}{f_y} \tag{37}$$

$$\lambda_s = \begin{Bmatrix} 1.60 - 0.75\alpha_s & 0.20 \leq \alpha_s \leq 0.50 \\ 1.35 - 0.25\alpha_s & 0.50 \leq \alpha_s \leq 1.00 \\ 1.20 - 0.10\alpha_s & 1.00 \leq \alpha_s \leq 2.50 \\ 1.30 - 0.14\alpha_s & 2.50 \leq \alpha_s \leq 5.00 \end{Bmatrix} \tag{38}$$

$$v_{max} = \frac{V_g}{A_c} + \frac{\gamma_v M_{unb}}{J_c}e \tag{39}$$

$$\gamma_v = 1 - \gamma_f \tag{40}$$

$$\gamma_f = \frac{1}{1+(\frac{2}{3})\sqrt{b_1/b_2}} \tag{41}$$

$$V_{max} = V_g + \frac{\gamma_v A_c e}{J_c}M_{unb} \tag{42}$$

1.2 Eccentric Shear Stress Model for Combined Shear and Moment Transfer

The behaviour and, consequently, the analysis of eccentrically loaded slab-column connections becomes significantly more complex with the introduction of unbalanced moments. Such loading cases arise when the slab-column connection is subjected to asymmetrical loading (gravity or lateral) and/or unequal slab spans, and result in a combination of flexure, shear, and torsion transferred from the slab to the column.

The traditional ACI design method, commonly referred to as the J_c Method, is based on a linear variation of shear stress and is implemented in both CSA S806-12 (Canadian Standards Association, 2012) and ACI 318-11 (ACI Committee 318, 2011). The maximum shear stress, v_{max}, acting on the critical section is given by Equation **39**, where V_g is the

factored direct shear force due to vertical loads, A_c is the critical shear section area (product of b_o, the length of the critical shear perimeter measured a distance $d/2$ from the column face, and d, the effective slab depth), γ_v is the fraction of the factored unbalanced moment, M_{unb}, that is being transferred to the critical shear section through shear stresses, J_c is a geometric property of the critical shear section analogous to the polar moment of inertia, and e is the distance between the centroid of the critical shear section and the location of the maximum shear stress.

Intuitively, in the absence of supporting beams or spandrels, all the applied loads acting on the slab must be transferred directly to the column, and thus the sum of the moment transferred by shear and that transferred by flexure must equal the total unbalanced moment being applied to the connection. This is expressed by Equation **40**, where γ_f is the fraction of the factored unbalanced moment, M_{unb}, transferred to the critical shear section by direct flexure, and is solely a function of the geometric properties of the column as shown in Equation **41**.

It can easily be shown that for an interior column with square geometry ($b_1 = b_2$), Equation **41** reduces to $\gamma_f = 0.60$; that is, 60% of the unbalanced moment is assumed to be transferred by flexure and the remaining 40% to be transferred by shear (Wight & MacGregor, 2011).

The eccentric shear stress model assumes that the shear stresses acting on the critical shear perimeter vary linearly with the distance from the centroidal axis of the critical perimeter. The total combined shear stress is taken to be the superposition of the direct shear stresses and the fraction of the unbalanced moment transferred by shear. To gain insight into Equation **39**, both sides can be multiplied by the critical shear section area, $A_c = b_o d$, to yield Equation **42**. When expressed in this form, it can be easily recognized that the eccentric shear stress model is nothing more than a linear equation having a y-intercept equal to V_g and slope equal to $\gamma_v A_c e/J_c$. Note that the slope in Equation **42** is an invariable number that is a function of the geometric properties of the slab-column connection, and, as a result, the maximum shear stress increases proportionally with the magnitude of the applied unbalanced moment (Song et al., 2012).

2 Methods

Data from 39 interior and edge slab-column connections were collected from published literature (El-Gendy & El-Salakawy, 2015; El-Ghandour et al., 1999, 2003; Gouda & El-Salakawy, 2015; Ospina et al., 2003; Hussein et al., 2004; Zaghloul & Razaqpur, 2004; Lee et al., 2009; Dulude et al., 2010; Nguyen-Minh & Rovňák, 2013). All the chosen specimens met the following selection criteria: (1) GFRP-reinforced two-way flat plates, (2) compressive concrete strength < 60 MPa, (3) square column geometry, (4) monotonic loading, (5) no transverse shear reinforcement, and (6) singly-reinforced with reinforcement in tensile zone only.

The three major code equations and eight proposed prediction models were applied to both concentrically and eccentrically loaded interior and edge connections. All reduction factors and safety factors were set equal to 1.00 during the analysis to predict the nominal punching shear strength. Also, the test-to-predicted shear strength ratio is presented for every equation. Three conclusions can be made based on the value of this ratio: (1) if $V_{TEST}/V_{PRED} = 1$, the model or code perfectly predicts the ultimate punching shear capacity; (2) if $V_{TEST}/V_{PRED} < 1$, the model or code overestimates the ultimate punching shear capacity; (3) if $V_{TEST}/V_{PRED} > 1$, the model or code underestimates the ultimate punching shear capacity. Therefore, based on the three cases mentioned above, the most desirable case is when the test-to-predicted ratio approaches unity.

3 Results & Discussion

3.1 Interior Specimens Concentrically Loaded

The test-to-predicted shear ratios are summarized in Table 1 for 29 interior connections. Note that two design provisions, ACI 318-05 (ACI Committee 318, 2005) and BS 8110-97 (British Standards Institution, 1997), are valid for steel-RC slab-column connections only and so serve as a reference.

The ACI guideline Equation **4** produced highly conservative results, with a mean of 2.003 and standard deviation of 0.276 (coefficient of variation (COV) = 13.76%). The design provision was developed based on the one-way shear equation proposed by Tureyen & Frosch (2003) and assumes that only the uncracked concrete contributes to the resistance of shear stresses. It completely neglects the contribution from the aggregate interlock and the dowel action of the reinforcing bars and therefore significantly underestimates the strength of the connection. The Canadian standard (Equation **1**–Equation **3**) and Japanese standard (Equation **6**) produce more accurate results of 1.046 ± 0.142 (COV = 13.60%) and 1.127 ± 0.163 (COV = 14.47%), respectively. Based on this sample group, the Canadian standard CSA S806 (Canadian Standards Association, 2012) is more accurate than the Japanese standard (Japan Society of Civil Engineering, 1997) at predicting the punching shear strengths of concentrically loaded interior slab-column connections reinforced with

Table 1: *Comparison between experimental and predicted strength for concentrically loaded interior slab-column connections from published literature.*

Code Provision (Equation #)	V_{TEST}/V_{PRED}		
	Mean	Std. Dev.	COV (%)
ACI 318[a] (14)	0.834	0.225	27.01
BS 8110[a] (12)	0.775	0.138	17.80
ACI 440 (4)	2.003	0.276	13.76
CSA S806 (Min 1-3)	1.046	0.142	13.60
JSCE 97 (6)	1.127	0.163	14.47
El-Ghandour et al. (15)	1.280	0.292	22.84
Matthys and Taerwe (18)	1.143	0.164	14.37
Ospina et al. (19)	0.978	0.153	15.64
El-Gamal et al. (21)	0.999	0.153	15.31
Theodorakopoulos and Swamy (23)	1.000	0.122	12.25
Zaghloul and Razaqpur (20)	0.905	0.123	13.61
IStructE (13)	1.194	0.172	14.37
El-Ghandour et al. (17)	0.955	0.137	14.37

[a] Code provision for steel-RC slab-column connections only.

GFRP. All three code provisions tend to underestimate, to varying degrees, the punching shear capacity. All the average test-to-predicted punching shear strengths lie above 1.00, indicating that the predicted capacity is less than the observed capacity, and thus are suitable for design purposes.

Both the Canadian standard and Japanese standard take the cubic root of the axial stiffness, $(\rho_f E_f)^{1/3}$, in their prediction equations. Additionally, the Canadian standard takes the cubic root of the compressive strength of concrete, whereas the Japanese standard takes the square root and imposes a limit on its design compressive strength. The governing CSA equation was always Equation **3**. For Equation **1** and Equation **2** to govern, the column aspect ratio, β_c, must be larger than 2 or the critical perimeter to effective slab depth, b_o/d, must be less than 20, respectively. However, the Japanese standard considers the effect of the slab size, reinforcement type and ratio, and column size by introducing three parameters, β_d, β_p, and β_r, respectively. Thus, the effect of these parameters is included in every prediction made by the Japanese design equation, whereas they are only included in the Canadian standard if they satisfy the specific constraints.

Equation **13** (IStructE, 1999), Equation **15** (El-Ghandour et al., 2000), and Equation **18** (Matthys & Taerwe, 2009) all produce underestimated capacities, whereas Equation **17** (El-Ghandour et al., 2000) and Equation **20** (Zaghloul & Razaqpur, 2004) yield overestimated predictions. Equation **19** (Ospina et al., 2003), Equation **21** (El-Gamal et al., 2005), and Equation **23** (Theodorakopoulos & Swamy, 2002) produce accurate predictions with average V_{TEST}/V_{PRED} ratios approximately equal to 1.00. Equation **15** (El-Ghandour et al., 2000) introduced the term $(E_f/E_s)^{1/3}$ into Equation **14** (ACI Committee 318, 1995) to develop their first model. Comparison of the results from Equation **14** and Equation **15** shows minor improvements. The unmodified Equation **14** does not produce conservative design results (predicted strength > test strength) with a mean of 0.834, whereas the modified ACI 318-05 (Equation **15**) (El-Ghandour et al., 2000) yields conservative results with a mean of 1.280. The introduction of the above term in Equation **14** results in a slightly larger standard deviation, but a lower COV.

ACI 318-05 (Equation **14**) (ACI Committee 318, 1995) was further refined by El-Gamal et al. (2005) (Equation **21**) by considering the axial stiffness of the bottom tensile reinforcement and the continuity of the slab. The authors showed that the punching shear strength is influenced by lateral constraints and boundary conditions. It was observed that the punching shear capacity of a slab is enhanced when it is restrained by adjacent slabs, as the slab edges are restricted from movement. The results of this analysis proved to support the modifications made by El-Gamal et al. (2005), yielding 0.999 ± 0.153 (COV = 15.31%). This is a significant improvement from the results produced by Equation **14** and Equation **15**.

Table 2: *Comparison between experimental and predicted strength for eccentrically loaded interior slab-column connections from Gouda & El-Salakawy (2015).*

Code Provision (Equation #)	V_{TEST}/V_{PRED}		
	Mean	Std. Dev.	COV (%)
ACI 318[a] (14)	0.820	0.136	16.56
BS8110[a] (12)	0.765	0.039	5.11
ACI 440 (4)	1.890	0.115	6.07
CSA S806 (Min. 1-3)	1.005	0.051	5.11
JSCE 97 (6)	1.126	0.074	6.59
El-Ghandour et al. (15)	1.174	0.194	16.56
Matthys and Taerwe (18)	1.049	0.054	5.11
Ospina et al. (19)	0.804	0.041	5.11
El-Gamal et al. (21)	0.926	0.083	8.94
Theodorakopoulos and Swamy (23)	0.917	0.053	5.76
Zaghloul and Razaqpur (20)	0.869	0.044	5.10
IStructE (13)	1.096	0.056	5.11
El-Ghandour et al. (17)	0.876	0.045	5.11

[a] Code provisions for steel-RC slabs only.

The current American guideline (Equation 4) for the ultimate punching shear of concrete slabs reinforced with GFRP bars or grids possesses the same form as that of ACI 318-05 (Equation 14). ACI 440 (Equation 4) considers the effect of reinforcement stiffness (axial stiffness) by means of calculating a cracked transformed section NA depth. This NA depth is a function of the flexural reinforcement ratio of the GFRP reinforcement as well as the modular ratio, the ratio of elastic modulus of GFRP to elastic modulus of concrete. Equation 21, proposed by El-Gamal et al. (2005), better represents the punching shear of concentrically loaded interior connections, in comparison to the current standard used in practice by ACI 440 (ACI Committee 440, 2015). All equations discussed above take the critical shear perimeter to be located at a distance of $d/2$ from the column face.

The British standard (Equation 12) applied directly to GFRP specimens underestimates the punching shear capacity, as expected based on the results of directly applying the ACI 318-05 code. Therefore, both steel codes yield higher predicted strengths compared to the actual or test strengths.

The British standard was first modified by Matthys & Taerwe (Equation 18) to account for the axial stiffness of the GFRP reinforcing bars. A substitution was made in the British standard for an equivalent steel ratio, $\rho_s = \rho_f E_f / E_s$. The effect of this substitution results in more accurate predictions of the punching shear (1.143 ± 0.164, COV = 14.37%). Ospina et al. (Equation 19) then modified the equation of Matthys & Taerwe (Equation 18) by taking the square root of the modular ratio E_f/E_s, instead of the cubic root. This improved the test-to-predicted ratio and slightly reduced the standard deviation, however an increase in the COV was observed. The Institute of Structural Engineers, UK (Equation 13) also proposed making the substitution in the British standard with an equivalent area of steel. El-Ghandour et al. (2000) proposed a second model (Equation 17) that introduced a different equivalent steel reinforcement ratio which imposes a strain limit of 0.0045 for GFRP. This substitution into the British standard yielded a mean of 0.955 ± 0.137 (COV = 14.37%). Comparison between the results from the Institute of Structural Engineers, UK (Equation 13) and El-Ghandour et al. (Equation 17), shows that the equivalent steel ratio proposed by El-Ghandour et al. (2000) produces results closer to the desired value of 1.00 and reduces the standard deviation slightly, with the COV remaining constant. For this set of equations discussed, the location of the critical shear perimeter is based on the British standard, and so measured a distance $1.5d$ from the column perimeter.

Zaghloul & Razaqpur (Equation 20) based their proposed equation on the one-way shear equation in the Canadian standard CSA S806-02 (Canadian Standards Association, 2012) and takes into consideration the axial stiffness of the reinforcing bars. This produced overestimated results with a mean of 0.905 ± 0.123 (COV = 13.61%). Of the 13

Table 3: *Comparison between experimental and predicted strength for eccentrically loaded edge slab-column connections from El-Gendy & El-Salakawy (2015).*

Code Provision (Equation #)	V_{TEST}/V_{PRED}		
	Mean	Std. Dev.	COV (%)
ACI 318[a] (14)	0.947	0.156	16.45
BS8110[a] (12)	0.877	0.076	8.62
ACI 440 (4)	2.073	0.209	10.08
CSA S806 (Min. 1-3)	1.206	0.129	10.72
JSCE 97 (6)	1.147	0.135	11.78
El-Ghandour et al. (15)	1.412	0.231	16.39
Matthys and Taerwe (18)	1.251	0.107	8.55
Ospina et al. (19)	0.978	0.083	8.51
El-Gamal et al. (21)	0.870	0.090	10.39
Theodorakopoulos and Swamy (23)	1.096	0.100	9.14
Zaghloul and Razaqpur (20)	0.968	0.104	10.72
IStructE (13)	1.307	0.112	8.55
El-Ghandour et al. (17)	1.045	0.089	8.55

[a] Code provisions for steel-RC slabs only.

equations compared, the analytically derived model of Theodorakopoulos & Swamy (Equation **23**) proved to be the most accurate. It was found that for the 29 slabs analyzed, the mean of the test-to-predicted punching shear strengths was 1.000 ± 0.122 (COV = 12.25%). This model possessed the smallest standard deviation and COV among all the equations tested, in addition to the mean being closest to 1.00. This model considers size effect as well as bond-slip between the GFRP reinforcement and concrete. Additionally, it considers the compressive strength of concrete and flexural reinforcement ratio to be co-dependent entities, not isolated entities as suggested by the other prediction equations.

3.2 Interior Specimens Eccentrically Loaded

These equations were applied to the eccentrically loaded interior slab-column connections tested by Gouda & El-Salakawy (2015). The flexural reinforcement ratio of the connections ranged from 0.65% to 1.30% and the moment-to-shear ratio M/V was constant at 150 mm for all specimens. Table 2 presents the results of each equation by listing their mean V_{TEST}/V_{PRED} value, standard deviation, and COV.

Comparison of the three major code provisions depicts a similar trend as witnessed by the concentrically loaded interior connections. Specifically, the American guideline (Equation **4**) produces highly overestimated predictions with V_{TEST}/V_{PRED} = 1.890 ± 0.115 (COV = 6.07%); whereas the Canadian standard (Equation **1**–Equation **3**) and Japanese standard (Equation **6**) yield slightly overestimated predictions with V_{TEST}/V_{PRED} = 1.005 ± 0.051 (COV = 5.11%) and V_{TEST}/V_{PRED} = 1.126 ± 0.074 (COV = 6.59%), respectively. The standard deviation and COV are significantly lower for the eccentrically loaded interior connections than for the concentrically loaded interior connections, as is expected from a smaller sample size. This must be taken into consideration when comparing the results from each equation as it would be misleading to assume that the code equations yield better results for eccentric loading than concentric loading until further testing has been conducted.

El-Ghandour et al. (Equation **15**), Matthys & Taerwe (Equation **18**), and IStructE (Equation **13**) predict mean V_{TEST}/V_{PRED} values greater than 1.00, as they did for the concentrically loaded specimens. Moreover, the degree of conservatism is approximately the same for both concentrically and eccentrically loaded connections. The remaining equations yield overestimated results by predicting a punching shear strength greater than the observed punching shear strength. The three most accurate equations of the concentric analysis predicted under conservative strengths for the eccentric group. Of the equations, Matthys & Taerwe (Equation **13**) exhibited the most accurate predictions with V_{TEST}/V_{PRED} = 1.049 ± 0.054 (COV = 5.11%).

3.3 Edge Specimens Eccentrically Loaded

The edge specimens of El-Gendy & El-Salakawy (2014) had

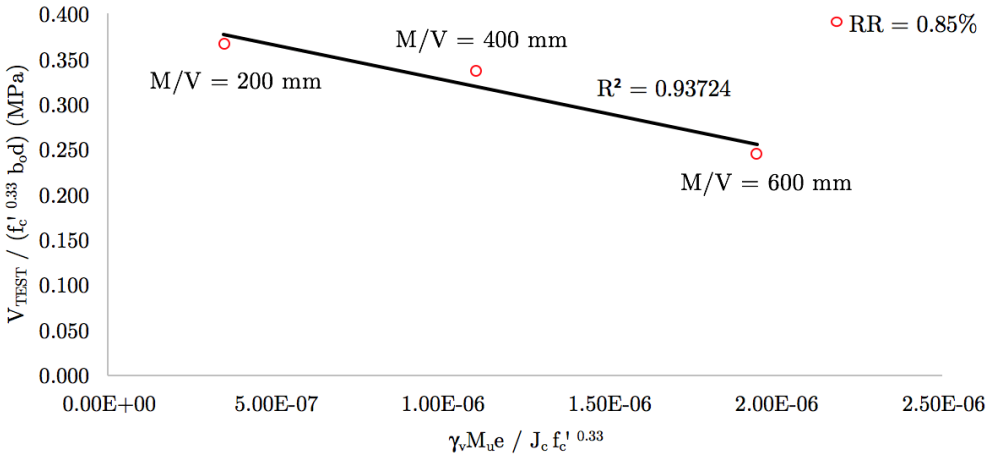

Figure 1: *Effect of moment-to-shear ratio on normalized shear strength.*

flexural reinforcement ratios ranging from 0.85% to 1.70%. Unlike the specimens of Gouda & El-Salakawy (2015), the moment-to-shear ratio M/V varied from 200 mm to 600 mm. Comparison of the previous results with those above shows that many of the proposed prediction equations yielded inconsistent, and in some cases very unsafe, predictions for connections subjected to combined moment and shear transfer. For instance, the most accurate prediction model for concentric loading was found to be that proposed by Theodorakopoulos & Swamy (Equation 23) with V_{TEST}/V_{PRED} = 1.000 ± 0.122 (COV = 12.25%). However, when applied to eccentrically loaded interior (Table 2) and edge (Table 3) columns V_{TEST}/V_{PRED} = 0.917 ± 0.053 (COV = 5.76%) and V_{TEST}/V_{PRED} = 1.096 ± 0.100 (COV = 9.14%), respectively. This suggests that the proposed prediction equations require further modification to be applied safely and reliably to eccentrically loaded slab-column connections.

Three edge specimens were plotted against the unbalanced moment in Figure 1. The coefficient of determination, R^2, was calculated to be 94%. This suggests, therefore, that there is a linear relationship between the moment-to-shear ratio and the normalized punching shear strength. More specifically, the normalized punching shear strength decreases linearly as the moment-to-shear ratio is increased, as assumed by the eccentric shear stress model. This relationship thus validates the assumption of a linear variation in shear stress for flat plates reinforced with GFRP.

4 Conclusion

The following conclusions can be drawn from the comparative study discussed above:

1. CSA S806-12 and JSCE-97 are applicable to GFRP-reinforced connections subjected to eccentric loading;
2. ACI 440-15 highly underestimates the capacity of slab-column connections as it neglects the contribution of the aggregate interlock and dowel action;
3. Many of the proposed equations yield inconsistent, and in some cases unsafe, predictions for interior and edge connections;
4. Results for edge connections support the assumption of a linear stress variation proposed by the eccentric shear stress model;
5. The equivalent steel ratio proposed by El-Ghandour et al. (2000) produced more accurate results than the ratio proposed by the Institute of Structural Engineers, UK (1999).

5 Recommendations for Future Work

Further investigation is warranted to study the effect of the following on the punching shear strength of eccentrically loaded interior, edge and corner connections:

1. Type of reinforcement, including Aramid-, Basalt-, and Carbon-fibre-reinforced polymer, and their respective bond characteristics;
2. Use of HSC;
3. Use of transverse shear reinforcement; and
4. Size effect.

6 Acknowledgements

Firstly, I would like to express my sincerest gratitude to Dr. Ehab El-Salakawy. Throughout my undergraduate degree, Dr. El-Salakawy has shared with me his knowledge and insight regarding the field of reinforced concrete structures and the implementation of GFRP composites as a reinforcing material. It was my privilege to be under his supervision and guidance.

I would also like to acknowledge Mohammed El-Gendy for his continuous support, encouragement, and advice. Mohammed's ability to clearly convey his ideas and expertise in a safe and welcoming environment is what I believe distinguishes him from other academic mentors. He was always happy to offer his help, even if it meant less time for his own work. For that, I am extremely grateful.

References

ACI Committee 318. (1995). *Building code requirements for structural concrete: ACI 318-95.* Detroit, MI, USA: American Concrete Institute.

ACI Committee 318. (2005). *Building code requirements for structural concrete and commentary & PCA notes on 318-05: ACI 318-05.* Detroit, MI, USA: American Concrete Institute.

ACI Committee 318. (2011). *Building code requirements for structural concrete and commentary: ACI 318-11.* Detroit, MI, USA: American Concrete Institute.

ACI Committee 440. (2015). *Guide for the design and construction of structural concrete reinforced with fiber-reinforced polymer bars: ACI 440.1R-15.* Detroit, MI, USA: American Concrete Institute.

British Standards Institution. (1997). *Structural use of concrete - code of practice for design and construction.* London, UK: British Standards Institution.

Canadian Standards Association. (2002). *Design and construction of building components with fibre-reinforced polymers, CAN/CSA 806-02.* Toronto, ON, Canada: Canadian Standards Association.

Canadian Standards Association. (2004). *Design of concrete structures, CAN/CSA A23.3-04.* Toronto, ON, Canada: Canadian Standards Association.

Canadian Standards Association. (2012). *Design and construction of building structures with fibre-reinforced polymer, CAN/CSA S806-12.* Toronto, ON, Canada: Canadian Standards Association.

Dulude, C., Ahmed, E., & Benmokrane, B. (2010). Punching shear strength of concrete flat slabs reinforced with GFRP bars. *2nd International Structures Specialty Conference, Winnipeg, MB, Canada*, 1-9.

El-Gamal, S., El-Salakawy, E. F., & Benmokrane, B. (2005). A new punching shear equation for two-way concrete slabs reinforced with FRP bars. *ACI Special Publication*, *230*, 877-894.

El-Gendy, M., & El-Salakawy, E. F. (2014). Punching shear behaviour of edge slab-column connections reinforced with FRP composite bars. *7th International Conference on FRP Composites in Civil Engineering (CICE 2014), August 20-22, Vancouver, BC, Canada.*

El-Gendy, M., & El-Salakawy, E. F. (2015). GFRP-RC slab-column edge connections with GFRP shear studs. *12th International Symposium on RFP For Reinforced Concrete Structures (FRPRCS-12) & the 5th Asia-Pacific Conference on FRPs in Structures (APFIS-2015) Joint Conference, 14-16 December 2015, Nanjing, China.*

El-Ghandour, A. W., Pilakoutas, K., & Waldron, P. (1999). New approach for punching shear capacity prediction of fiber reinforced polymer reinforced concrete flat slabs. *ACI Special Publication*, *188*, 135-144.

El-Ghandour, A. W., Pilakoutas, K., & Waldron, P. (2000). Punching shear behavior and design of FRP RC slabs. *Proceedings of the International Workshop on Punching Shear Capacity of RC Slabs, Stockholm, Sweden*, 359-366.

El-Ghandour, A. W., Pilakoutas, K., & Waldron, P. (2003). Punching shear behavior of fiber reinforced polymers reinforced concrete flat slabs: Experimental study. *Journal of Composites for Construction*, *7*(3), 258-265.

Gouda, A., & El-Salakawy, E. F. (2015). Finite element modeling on interior slab-column connections reinforced with GFRP bars subjected to moment transfer. *Fibers*, *3*, 411-431.

Gu, X., Jin, X., & Zhou, Y. (2016). *Basic principles of concrete structures.* Berlin, Germany: Springer-Verlag.

Hussein, A., Rashid, I., & Benmokrane, B. (2004). Two-way concrete slabs reinforced with gfrp bars. *4th International Conference on Advanced Composite Material in Bridges and Structures, Calgary, AB, Canada*, 1-8.

IStructE. (1999). *Standard method of detailing structural concrete: A manual for best practice.* London, UK: The Institution of Structural Engineers.

Japan Society of Civil Engineering. (1997). *Recommendation for design and construction of concrete structures using continuous fibre reinforcing materials: Concrete engineering series 23.* Tokyo, Japan: Japan Society of Civil Engineering.

Lee, J. H., Yoon, Y. S., Cook, W. D., & Mitchell, D. (2009). Improving punching shear behavior of glass fiber-reinforced polymer reinforced slabs. *ACI Structural Journal*, *106*(4), 427-434.

Matthys, S., & Taerwe, L. (2009). Concrete slabs reinforced with FRP grids. II: Punching resistance. *Journal of Composites for Construction*, *4*(3), 154-161.

Nguyen-Minh, L., & Rovňák, M. (2013). Punching shear resistance of interior GFRP reinforced slab-column connections. *Journal of Composites for Construction*, *17*(1), 2-13.

Ospina, C. E., Alexander, S. D. B., & Cheng, J. J. R. (2003). Punching of two-way concrete slabs with fiber-reinforced polymer reinforcing bars or grids. *ACI Structural Journal*, *100*(5), 589-298.

Song, J.-K., Kim, J., Song, H.-B., & Song, J.-W. (2012). Effective punching shear and moment capacity of flat plate-column connection with shear reinforcements for lateral loading. *International Journal of Concrete Structures and Materials*, *6*(1), 19-29.

Theodorakopoulos, D. D., & Swamy, N. (2007). Analytical model to predict punching shear strength of FRP-reinforced concrete flat slabs. *ACI Structural Journal*, *104*(3), 257-266.

Theodorakopoulos, D. D., & Swamy, R. N. (2002). Ultimate punching shear strength analysis of slab-column connections. *Cement and Concrete Composites*, *24*, 509-521.

Theodorakopoulos, D. D., & Swamy, R. N. (2008a). A design model for punching shear of FRP-reinforced slab-column connections. *Cement & Concrete Composites*, 544-555.

Theodorakopoulos, D. D., & Swamy, R. N. (2008b). Analytical model to predict punching shear strength of frp-reinforced concrete flat slabs. *ACI Structural Journal*, *104*, S25.

Tureyen, A., & Frosch, R. (2003). Concrete shear strength: Another perspective. *ACI Structural Journal*, *100*(5), 609-615.

Wight, J. K., & MacGregor, J. G. (2011). *Reinforced concrete: Mechanics and design*. Boston, MA, USA: Prentice Hall.

Zaghloul, A., & Razaqpur, A. (2004). Punching shear strength of concrete flat plates reinforced with CFRP grids. *Proceedings of the 4th Conference on Advanced Composite Materials in Bridges and Structures, Calgary, AB, Canada*, 1-8.